Pol. J. Environ. Stud. Vol. 34, No. 5 (2025), 6163-6176
DOI: *10.15244/pjoes/191975* ONLINE PUBLICATION DATE: 2024-10-21

Original Research

Eco-Friendly Approach for Synthesis of Silver Nano-Particles Using Aqueous Leaf Extract of *Kalanchoe pinnata* as Antimicrobial Agents

Mansi Guleriya[1], Somya Sinha[1]*, Kumud Pant[1], Prateek Gururani[1], Nilay Singh[1], Janhvi Mishra Rawat[1], Naveen Chandra Joshi[2], Sarah González Henao[3], Debasis Mitra[4], Rokayya Sami[5]***, Helal F. Al-Harthi[6], Roqayah H. Kadi[7], N.I. Aljuraide[8], Ruqaiah I. Bedaiwi[9]**

[1]Department of Biotechnology, Graphic Era (Deemed to be University), Dehradun, 248002 Uttarakhand, India
[2]Department of Research and Innovation, Uttaranchal University, Dehradun, 248007 Uttarakhand, India
[3]Department of Earth and Environmental Sciences, Department of Microbiology and Molecular Genetics, Michigan State University, East Lansing, MI, United States
[4]Department of Microbiology, Graphic Era (Deemed to be University), Dehradun, 248002 Uttarakhand, India
[5]Department of Food Science and Nutrition, College of Sciences, Taif University, P.O. Box 11099, Taif 21944, Saudi Arabia
[6]Department of Biology, Turabah University College, Taif University, 21995, Saudi Arabia
[7]Department of Biological Sciences, College of Science, University of Jeddah, Jeddah 21959, Saudi Arabia
[8]Department of Physics, Turabah Branch, Turabah University College, Taif University, P.O. Box 11099, Taif 21944, Saudi Arabia
[9]Department of Medical Laboratory Technology, Faculty of Applied Medical Sciences, University of Tabuk, Tabuk 71491, Saudi Arabia

Received: 6 April 2024
Accepted: 3 August 2024

Abstract

The utilization of plant extracts in the biogenic amalgamation of metallic silver nano-particles is a nature-friendly approach compared to the classical methods adopted earlier. The current study involved the bio-synthesis of AgNPs using *Kalanchoe pinnata* leaf extract. The presence of phyto-constituents in the leaf extract revealed the reducing ability of *Kp-AgNPs* followed by nucleation. Physicochemical characterization techniques *viz*. scanning electron microscope (SEM), Fourier-transform infrared spectroscopy (FTIR), transmission electron microscopy (TEM), UV-*vis* spectroscopy, electron diffraction studies, and zeta potential gave spectra at 400 nm with surface morphological features in the form of spherical AgNPs, detection of functional groups, and interaction between the particles in the aqueous leaf extract. Moreover, *Kp-AgNPs* were effective in inhibiting different bacterial strains. Hence, it can be inferred from this study that AgNPs have an inclusive range of applications, including the fabrication of biomedical, optical, and electronic devices.

Keywords: Silver Nanoparticles, Biofabrication, Physicochemical, Characterization, *K. pinnata*

*e-mail: somya12121993@gmail.com
**e-mail: debasismitra3@gmail.com
***e-mail: rokayya.d@tu.edu.sa

Introduction

Nanotechnology has attracted the attention of researchers over the past ten years, among which numerous types of nanoparticles have always been in the limelight of readers, among which silver nanoparticles have gained considerable importance [1]. Outstanding to the biological, physical, chemical, and optical characteristics and their extensive use in drug delivery in the form of topical creams & lotions, nanoparticles have found profound usage in the electrical, optical, food, and beverage industries, agricultural sectors, textile industry, and wastewater management [2]. In most studies and reviews [3–6], multiple physical, biological, and chemical processes have been described as ways to produce AgNPs. Each of these techniques varies in its number of benefits and drawbacks depending on how it is applied. For example, chemically produced nanoparticles (NPs) can be immediately employed for requirement analysis [7]. The development of antimicrobial agents and other alternative forms of medicine is driven by the rapid rise in drug resistance to existing antibiotics, increased likelihood of microbial infections, and rapid evolution *via* mutations [8–11]. Advances in nanotechnology have resulted in the fabrication of nano-particles with strong anti-bacterial properties that are effective against infections and drug resistance, providing a platform to fight against microbial transformation [12, 13]. Metal nanoparticles are used in some of the most cutting-edge nano-technological applications, and because of their distinct mode of action, they provide the most successful outcomes [14]. Ag nanoparticles at the nanoscale offer an improved surface volume ratio and are regarded as an interesting study when compared to other metals in their nanoscale ranges because of their powerful antimicrobial potential against bacterial and fungal strains [15–17]. Moreover, the methodology adopted for biofabrication is helpful against bacteria that are both multidrug sensitive and resistant, together with resistant (methicillin) *Staphylococcus aureus*, resistant (vancomycin) *S. aureus*, resistant (ampicillin) *Escherichia coli* and *Pseudomonas aeruginosa* [18]. AgNPs can be obtained from various medicinal plants [19, 20]. *Kalanchoe pinnata (Bryophyllum pinnatum*), a plant (medicinal) belonging to the *Crassulaceae* family, often referred to as patharchatta, has been used in Ayurvedic medicine since primeval times [21, 22]. This plant is widespread in countries, such as India, Hawaii, Australia, and tropical Africa. Plant parts, such as stems, roots, and leaves, are utilized for the formation of nano-particles. Alkaloids, flavonoids, phenolic compounds, and glycosides are among the molecular groups found in plants, which offer additional properties, mainly anti-bacterial, anti-inflammatory, anti-viral, anticancer [23], antilithic [24, 25], and wound healing properties [26]. The features of the nano-sized particles generated from plant extracts are influenced by a number of variables, like reaction duration, pH, and temperature, but the type of macromolecules in the phytochemistry may be an important element in the bioprocess [27–29]. Due to the existence of bio-reducing agents required for the synthesis viz. polyphenols, terpenes, flavonoids, carbohydrates, peptides, alkaloids, specific enzymes, and amino acids. Moreover, the chosen extract is important for understanding the concept of nanoparticle synthesis via plants [30]. A crucial aspect of environmentally friendly manufacturing of AgNPs is the decrease of silver ions in the $AgNO_3$ solution using plant extracts. Two distinct phases were identified in the process of preparation of nanoparticles: the nucleation period, during which the Ag ions use a high activation energy to form small nuclei, and the growth condition, during which the small nucleus is clustered and thus aids in the development

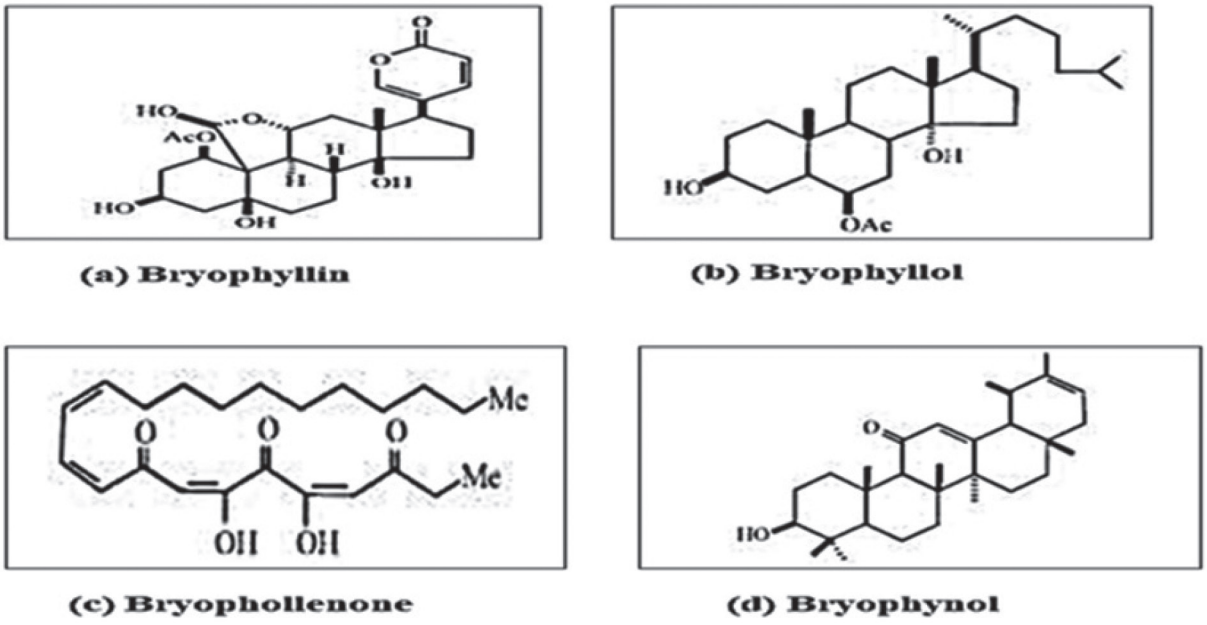

Fig. 1. Important phyto-active constituents of *K. pinnata.*

Fig. 2. *Kalanchoe pinnata.*

Fig. 3. Powder form of leaves.

of nanoparticles [31, 32]. Owing to the reduction potential of metallic Ag, chemically stable particles can be generated and synthesized in aqueous solutions [33–35], as shown in Fig. 1. In our study, silver nanoparticles (spherical) were fabricated using *K. pinnata* leaf extract and biological activity & physiochemical characterization techniques demonstrated the ability of *K. pinnata* to form AgNPs. In addition, the spectral characterization of the plant has been reported for its anti-bacterial activity against bacteria capable of retaining stains.

Materials and Methods

Phytochemical Constituents of *Kalanchoe Pinnata*

Flavonoids, glycosides, lipids, cardenolides, bufadienolides, triterpenes, steroids, and alkaloids were abundant in *K. pinnatum*. Bufadienolides, which are a group of active compounds, were abundant in the leaves (Fig. 2 and 3). Bufadienolides, such as bryotoxins A, B, and C, are functionally and structurally similar to two or more digoxins, cardiac glycosides, and digitoxins.

Extraction

Twigs of *K. pinnata* were first washed with running tap water and then brushed twice with double distilled water. The leaves were dried and ground, and a 100 mL methanol sample was dissolved in 13 g of *K. pinnata* powder overnight. Before filtering the extract, the fluid was macerated and collected in a glass bottle with a cork after being filtered using filter paper, and then poised in a glass container with a cork. To obtain the powder, methanol was evaporated in an oven for approximately an hour at 65°C. After the addition of 30 ml of distilled water, it was placed in a falcon tube and stored at 4°C, which resulted in the evaporation of methanol and was stored for future use.

Silver Nitrate Solution Preparation

1.69 mg of $AgNO_3$ was thoroughly mixed with distilled water (DW) in a volume of 100 ml volume to obtain a stock solution of 0.1M Ag nitrate solution from which 0.01 and 0.001 M working solutions were prepared, as shown in (Fig. 4 a and b).

Biosynthesis of AgNPs Using K. pinnata

An $AgNO_3$ solution (100 mL) was prepared, from which 30 ml of *Kalanchoe Pinnata* leaf extract solution was added dropwise at RT while agitating it. The mixture resulted in a dark brown precipitate immediately after the addition of the leaf extract. After adding 30 ml of the solution, a precipitate was obtained and incubated for 24 hours. The samples were quickly spun down for 30 min at a speed of approximately 4000 rpm for separation after the incubation periods. The mass that had separated was repeatedly cleaned with alcohol in order to eliminate any

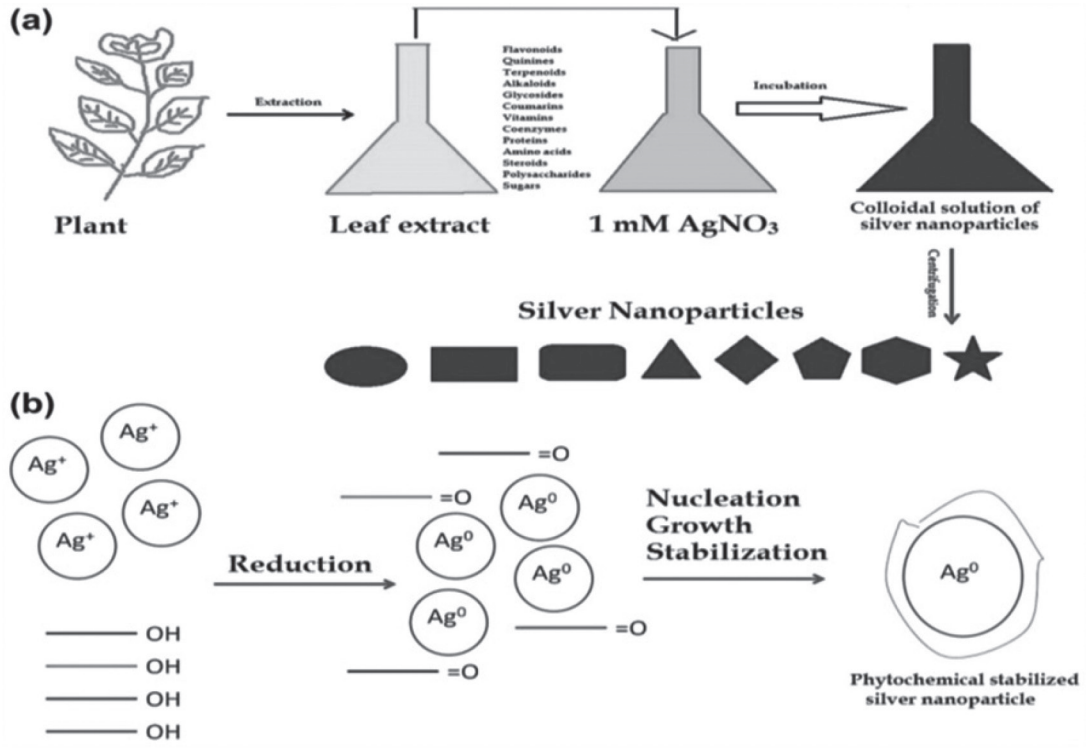

Fig. 4. (a) Schematic depiction of plant-mediated synthesis of AgNPs and (b) the process by which AgNPs are formed using a plant synthesis method.

organic impurities that were soluble in alcohol. The bulk solid was dried in an oven after thorough cleaning. The remaining solid material was completely dried to obtain a dark-colored material, which was ground into a powder using a mortar and pestle and tested for further characterization.

Physicochemical Characterization

Glass cuvettes and UV-Vis spectrophotometry were used to quantify the complete spectrum and study the reducing ability of Ag nitrate in aqueous solutions *via* plants. The spectrum of the solution was set between 300–700 nm, and the maximum absorbance was set to 4 L mol^{-1} cm^{-1}. The reaction mixture of the plant extracts and Ag^{+} ions in the solution underwent a color change, as observed by visual inspection. FTIR spectroscopy was utilized to explore the chemical-functional groups of the plant extract, which perform as a capping agent in the generation of AgNPs implicated in the bio-reduction of AgNPs in the 4000–650 per cm range with a resolution of 1.0 per cm. A particle size analyzer was used to identify the extent of particle design. The general configuration/ structure of AgNPs obtained using *Kalanchoe pinnata* was examined using a scanning electron microscope. All other investigations were conducted, and process-related supplements were used at room temperature. The change in color of the reaction mixture (plant extracts and Ag^{+} in the solution) was visualized.

UV-Visible Spectroscopy Analysis

The spectral characteristics of the bio-synthesized nanoparticles were examined using UV–visible spectroscopy. After the addition of deionized water to the solution mixture, spectra were obtained using a UV-2550 spectrophotometer, which operates at a resolution of 1 nm from 300 to 700 nm. For complete examination, UV-Vis spectrophotometry was used, in which distilled water was used as a control [36, 37]. Uncertainty surrounds the precise mechanism of extracellular production of metal NPs. According to this theory, Ag ions are neutralized by the NADH coenzyme, which acts as an electron shuttle [38, 39]. The estimated size of the visible nanoparticles was evaluated using the ImageJ-win32 program [40].

Zeta Potential

At 1-week intervals, the zeta potential of AgNPs was examined to determine their stability. Zeta potential values between -20 and -30 mV showed that the AgNPs were stable [41, 42].

Fourier Transform Infrared Spectroscopy (FTIR) Analysis

The presence of natural extracts or other related elements acts as a minimizing or capping agent on the surface of AgNPs, and was further evaluated using

FTIR. FTIR offers a wide range of benefits. The functional-groups present in a system can be understood in detail to identify the resonant frequencies of chemical bonds. The harmonic excitation energy of molecules, which is in the 1013–1014 Hz range, correlates with infrared radiation [43]. This implies that spectroscopic fluctuations of self-assembled functional groups connected to nanoparticle surfaces can be observed using IR spectroscopy for quantitative and qualitative investigation. FTIR allows investigation of the adsorption of functional-groups on the nanoparticles' surface [41]. FTIR measurements were performed using the reflection method on a Perkin Elmer Spectrum Spectrophotometer. Four FTIR analyses/scans in the frequency range 4000–650 cm^{-1} were carried out for each sample.

Stretching and bending vibrations (in the 4000–400 cm^{-1} area) were created by bonding with the produced molecules, which interacted with non-invasive IR radiation [12]. The involvement of the -CO-NH_2amide, -CO carbonyl, and -OH hydroxyl functional groups was revealed using FTIR spectral analysis (FTIR). Stretching and bending vibrations of the AgNPs (in the 4000–400 cm^{-1} area) were created when the bonding in the produced molecules interacted with noninvasive IR radiation [12]. The participation of amide (-CO-NH_2), carbonyl (-CO), and hydroxyl (-OH) functional groups in the process was further revealed by spectral analysis.

Scanning Electron Microscopy

On the gold-coated framework, a thin film of the sample was prepared by overlying a minor amount of sample on a grid, and the grid of the SEM was enabled to dry by placing it under a mercury (Hg) lamp for at least 10 min. The electron diffraction pattern of *Kp-AgNPs* was coated onto an EVO SEM (MA15/18) with a 51N1000–EDS System from Oxford Instruments Nano-analysis.

Transmission Electron Microscopy

A TECHNAI-G2–20-TWIN from FEI Company of USA (S.E.A.) PTE, Ltd. was employed with an Octane-Plus SDD Detector from EDAX Inc. For the TEM investigation, sample preparation was performed on a gold-coated TEM grid. The grid was recognized to set for two min, after which the *Kp-AgNPs* sample was separated using blotting paper, and the grid/ framework was dried under the IF lamp before quantification. The lucid appearance of the SAED pattern denotes the crystalline nature of the nanoparticles.

Nucleation of AgNPs at Various Reaction Rates

The fabrication of silver nanoparticles was indicated by a transformation in the coloration of the solution [30]. Numerous biomolecules, including flavonoids, phenols, and quinines, were found to be present in plant leaves and served as capping agents in the production and stability of AgNP solutions incubated for 15, 30, and 60 min. Biogenic AgNPs were found to have the highest absorbance at 400 nm, and the absorbance intensity units increased over time (2.363, 2.563, and 2.788 a.u.).

Anti-Bacterial Activity Assessment of *Kp-AgNPs*

The disc-diffusion technique was used to evaluate the antibacterial activity of the AgNPs. A variety of pathogenic bacterial strains, as well as *S. aureus* and *E. coli*, were inoculated in nutrient broth (HiMedia, India) and cultured for 24 h at 37°C in a shaking incubator. Bacterial cultures (100 µL) incubated overnight were evenly scattered across the surface of the plate containing the agar medium using a sterile L-shaped glass spreader. A sterile tweezer was used to gently insert spotlessly clean filter papers with a width of 25 mm that had been infused with the manufactured silver nanoparticles of varied concentrations over the surface of contaminated nutritional agar plates. The inhibition zone was measured in millimeters following a 24-hour incubation period at 37°C. The nanoparticle solutions were then impregnated with sterile discs measuring 6 mm in diameter at different concentrations (25 µL, 50 µL, and 75 µL). The Plates containing the impregnated discs were kept in the incubated for 24 h at 37°C. Ampicillin-containing commercial antibiotic discs were used as the controls. The zone of inhibition developed around the discs during incubation was measured using a ruler.

Results and Discussion

The color of the solvent continued to change throughout the reaction, which helped identify the biogenic development of silver nanoparticles. The bio-reduction of Ag particles was observed based on the color intensity due to the presence of *K. pinnata* leaf extract. The development of AgNPs was detected based on the surface plasmon resonance peak in UV-visible spectroscopy and the precipitation of particles with an altered solvent color.

Nucleation of AgNPs at Various Reaction Rates

On the addition of plant extract to the salt composed of Ag with a concentration of 1mM, the tint of the solution kept on changing. First, it underwent a transformation in color from light yellow coloration to pale yellow and then to dark brown as depicted in Fig. 5. The fabrication of silver nanoparticles was indicated by a change in the coloration of the solution [30]. Numerous biomolecules, including flavonoids, phenols, and quinines, have been found in plant leaves and serve as capping agents in the production and constancy of AgNPs. These were mainly responsible for converting Ag^+ NPs into Ag^0 NPs. AgNPs were found to be stable because the color of the solution was transformed to its maximum after 60 min and did not change further even after 24 h. AgNPs produced from *K. pinnata* leaves are shown in Fig. 5 by UV-visible spectroscopic analysis. AgNPs were detected to have a maximum absorption at

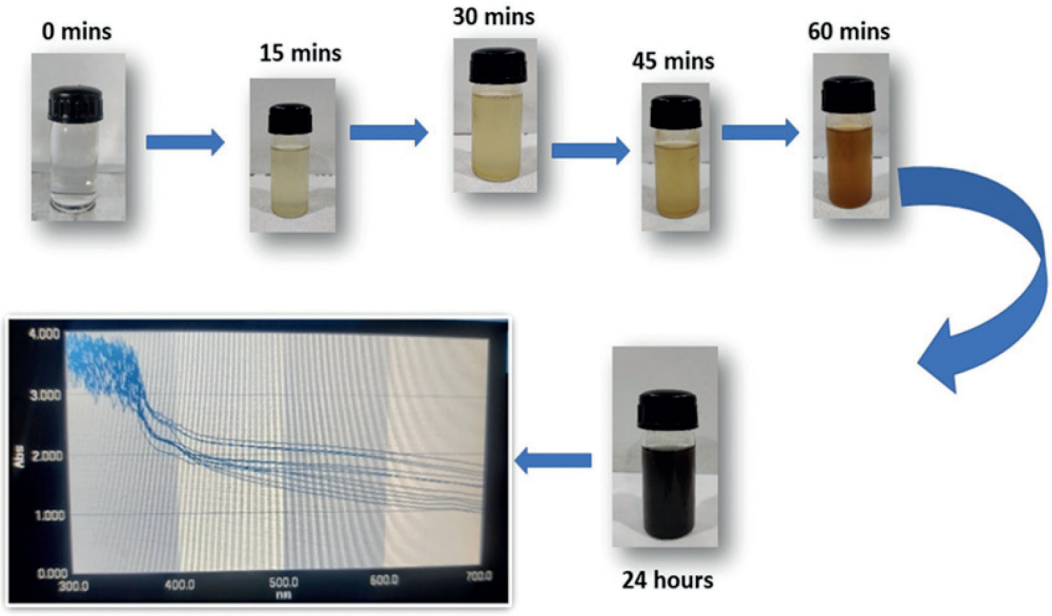

Fig. 5. Spectrum of Ag nanoparticles nucleation in the UV-visible range at various time intervals.

400 nm, and an increase in intensity indicated an increase in AgNP production over time. After incubation for 15, 30, and 60 min, the biogenic AgNPs were found to have the highest absorbance at 400 nm, and the intensity of the absorbance units improved over time (2.363, 2.563, and 2.788 a.u.). The wavelength at 400 nm did not vary during the course of the reaction at different timings. The color of the suspension began to change when AgNPs were formed in an aqueous solution containing the leaf extract of the plant. To conduct the trials, we used a synthesis process for 15 min, as shown in Fig. 5.

UV–Visible Spectroscopic Analysis

The dark brownish-black powder sample was diluted in deionized water and subsequently sonicated to avoid particle aggregation, so that the particles remained suspended. The mixture was then placed in a cuvette and subjected to UV-visible light, and the absorbance was measured. The interface plasmonic mechanism causes resonant peaks to form at various wavelengths for various nanoparticle solutions, which causes the maximum wavelength to be absorbed at the resonant wavelength. According to various research findings, normal AgNPs have typical electron excitation peaks at 350 nm and 475 nm. Surface absorbance is significantly influenced by several other factors, such as the size, structure, and inner distance of the particles formed in the media, as well as the solution (Fig. 6).

FTIR Analysis

FTIR spectral analysis was accomplished to evaluate the biological configuration of nanoparticles on the surface. The surface chemistry of AgNPs in *K. pinnata* leaf extract, which contains capping agents in the form of physiologically active compounds, was examined using infrared spectroscopy. Fig. 7 (a) and (b) display the spectra of the synthetic AgNPs and *K. pinnata* extract, respectively. Owing to the presence of carboxylic acid and the protein stretching vibrations of the plant-containing solution, a band was obtained at 3305.8 cm^{-1}. The vibration caused by the carbonyl group in the amide linkage of the proteins caused the detection of peaks at 1635.7 cm^{-1} and was related to the bending trembling of the amide [44, 45]. These findings suggest the existence and interaction of proteins with AgNPs, which plays a role in their synthesis and stabilization. *K. pinnata* leaf contains a variety of triterpene acids [46], flavonoids [47], sesquiterpene glycosides [48], polysaccharides, and proteins as per the phytochemical research reported. These elements have the potential to be used to convert Ag nitrate into AgNPs under the correct conditions, and they may also help stabilize AgNPs produced in the medium. This demonstrates that the capping role of secondary metabolites, which is responsible for the efficient creation of AgNPs, allows their development. According to this theory, modifying the surface plasmon resonance is caused by interactions between biomolecules, synthetic

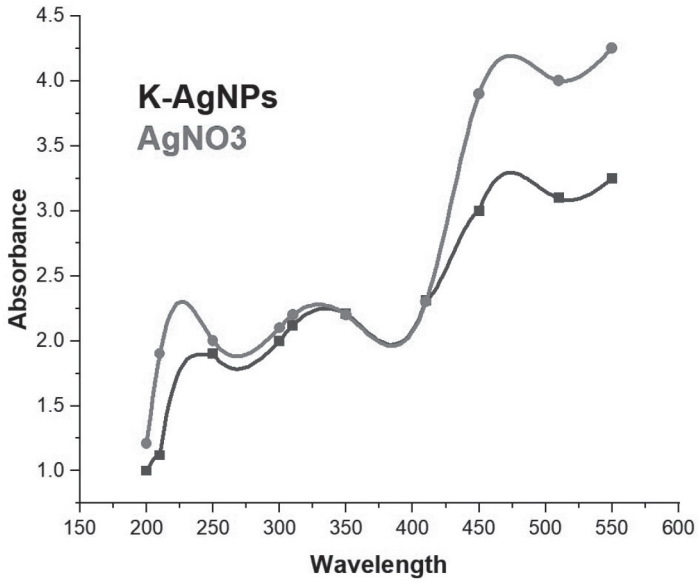

Fig. 6. UV-Vis spectroscopic analysis of *Kp-AgNPs.*

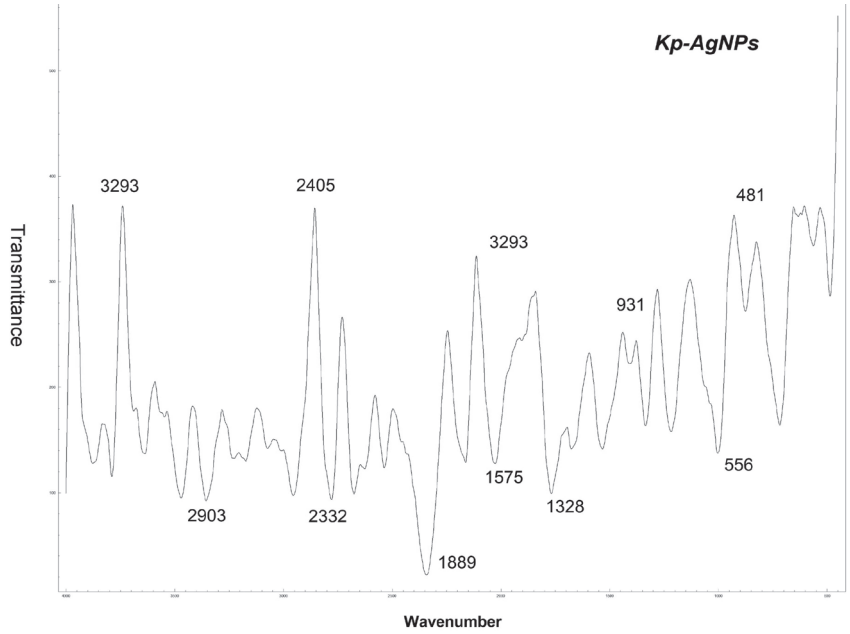

Fig. 7. FTIR spectrum of *Kp-AgNPs.*

nanoparticles, and phytochemicals. FTIR measurements and UV-vis spectroscopy confirmed the absorbance and particle size of the AgNPs. The AgNP-produced batches also revealed FTIR molecular profiles with distinct resonance bands (Fig. 7), and studies have shown that plant extracts are rich in secondary metabolites. The crystallinity of the biosynthesized AgNPs was evaluated to determine variations among the three batches.

Zeta Potential

The zeta potential affects the particle shape and suspension stability [49]. Owing to the electrostatic attraction and repulsive forces between the particles, a colloidal solution with a zeta potential of less than 30 mV is thought to be more stable [50]. The size and type of the surface charges associated with the double-layer

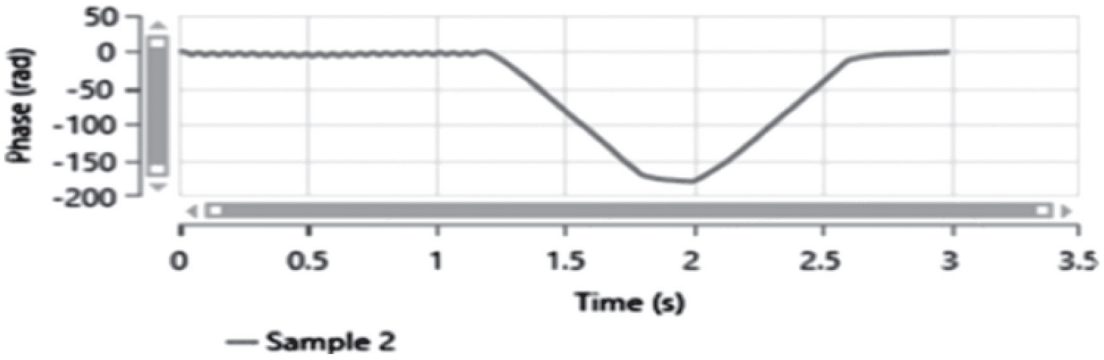

Parameters	Value
Z averageParticle Size	346 nm
Polydispersity Index	0.47
Zeta Potential (mV)	-27.48
Conductivity mS/cm	0.053
Quality Factor	4.96

Fig. 8. Particle Size and Zeta Potential of Kp-AgNPs.

encasing the particles were measured. It is affected by the ionic strength, pH, type of ions in the suspension, and particle size of the solution in the microenvironment [51]. The largest nanoparticles formed had a diameter of 37.8 nm and 43.8 nm. Fig. 8 shows the size distribution of the nanoparticles. The interactive value of the particles was found to be -26.7 mV and the average AgNP distribution in the colloidal solution indicated greater stability of the AgNPs and their hydrodynamic distribution. The specifics of the zeta potentials are shown in Fig. 8 highlighted in Sample 2.

Antimicrobial Activity of AgNPs

According to previous studies, the leaves of the herb *Bryophyllum pinnatum* are known to exhibit antibacterial characteristics [52, 53]. Phytochemicals, such as terpenoids, alkaloids, polyphenols, flavonoids, and organic acids (OC), present in the extract of *B. pinnatum* are responsible for its biological action, including its antimicrobial properties. The complex free radical species that bacteria produce when they interact with cell membranes affect each aspect of bacterial cell function [54, 55]. AgNPs synthesized from *B. pinnatum* leaf extract of *B. pinnatum* exhibited greater antibacterial activity. They also have stronger reactivity and smaller stable sizes, which contributes to their potential. The anti-bacterial effectiveness of AgNPs against both bacterial strains was assessed using the disc-diffusion technique [56]. Fig. 9 (a-d) illustrates the anti-bacterial activity of the AgNPs. The extent of the zone of inhibition that developed after 36 h at 37°C is evidence of the AgNPs' strong antibacterial activity. The *E. coli* zones of inhibition of gram-negative bacteria by *E. coli* are shown in Table 1. At various doses, AgNPs displayed a significantly greater zone of inhibition against both bacterial strains than that of the selected antimicrobial therapy. In the antibacterial experiment, the standard and control substances included silver salts. Owing to the smaller size of AgNPs compared to Ag nitrate and plant extract, their antibacterial activity was found to be superior. Smaller AgNPs can penetrate more bacterial cells, thereby expanding their zone of inhibition. The membrane of the bacterial cell breaks because of the electrostatic contact between positive charges, such as Ag^{+}, and -ve charges on the surface of the membrane. As AgNPs enter cells, they can alter their physicochemical properties, which are responsible for changes in the cellular structure, metabolism, and macromolecules, thereby impacting the overall functionality of the microbial cell. This can cause anomalies in physiological processes including respiration and cell permeability. Additionally, AgNPs interact with cellular macromolecules to generate various oxygen species that can harm cellular DNA, ultimately leading to cell death [57, 58].

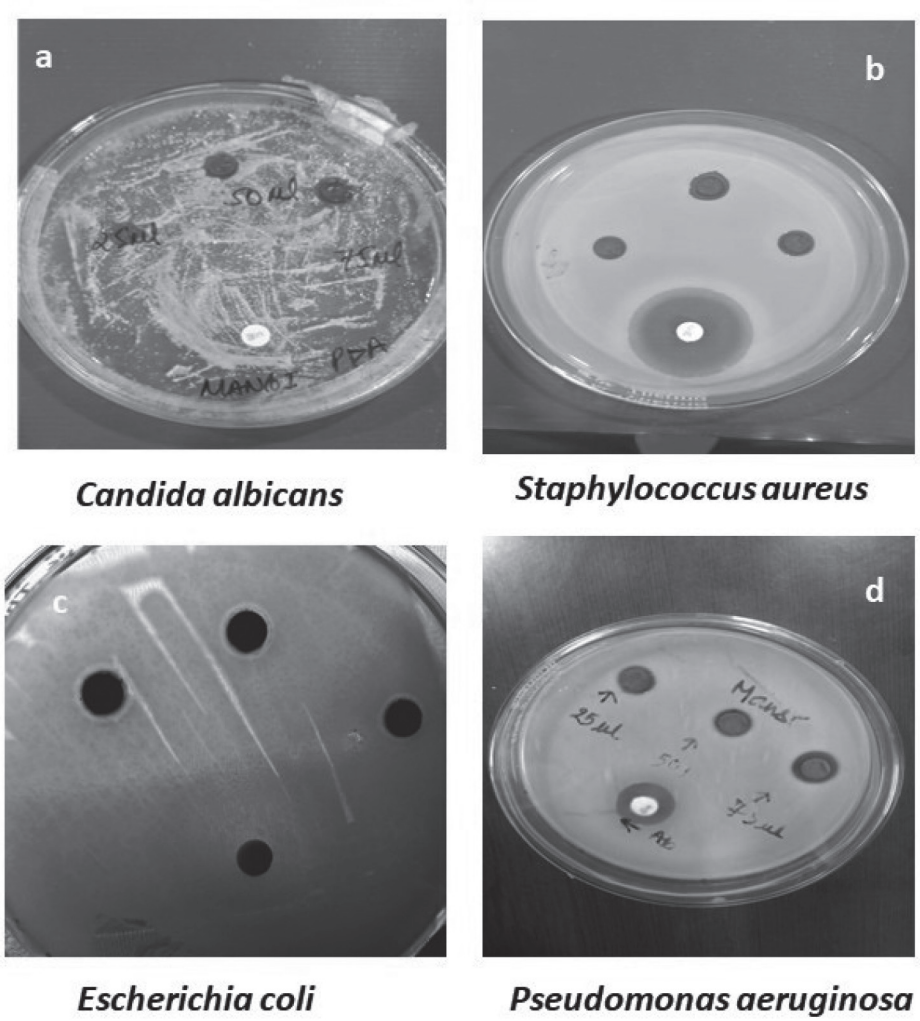

Fig. 9. Zone of inhibition of (a) *C. albicans*, (b) *S. aureus* (c*) E. coli* (d) *P. aeruginosa* treated with *Kp-AgNPs* (Here standard Drug in case of bacteria and fungi are streptomycin, chloramphenicol, and fluconazole respectively).

Table. 1. Zone of Inhibition for the synthesized *Kp-AgNPs* against Gram-Negative bacteria.

Pathogenic strain	Zone of Inhibition	Antibiotics
Staphylococcus aureus	8.60±2.1*	17 mm
Escherichia coli	12.5±0.36*	26.7 mm
Pseudomonas aeruginosa	6.89±0.47*	18 mm

Scanning Electron Microscopy

SEM measurements were used to illustrate the morphology and form of *Kp-AgNPs*. The largest size range of green *Kp-AgNPs* was observed in the range of 200 nm, and their structures were detected in various forms, as illustrated in Fig. 10 (a) and (b) at scales of 40 µm and 20 µm, respectively. These Figs. indicate the cuboidal, hexagonal, and rectangular shapes of *Kp-AgNPs* which were found to be significantly dispersed in nature. A few of the NPs in this group were found to be largely separated from one another, but the bulk was clumped together

Transmission Electron Microscopy

TEM was carried out using a TECHNAI 20G2 instrument at 200 KV to assess the morphology, size, and surface characteristics of biological samples. The synthesized *Kp-AgNPs* after 48 h are shown in Fig. 11 (a-c) are predominantly spherical. Further enlargement

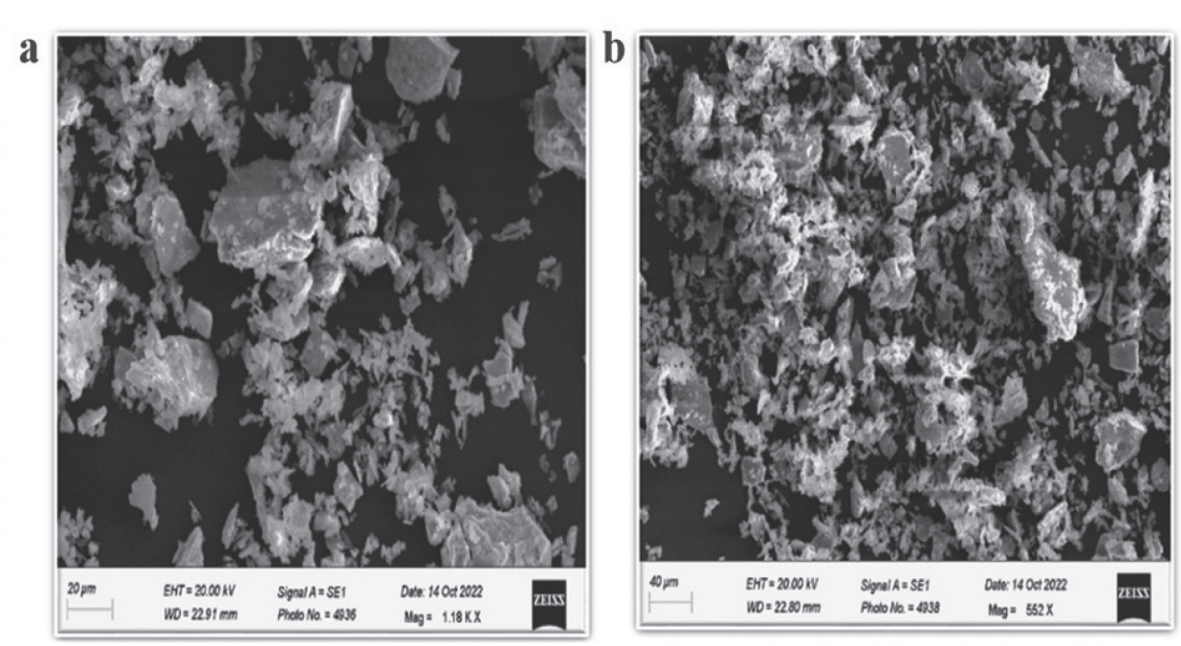

Fig 10. SEM images of *Kp-AgNPs* in the range of (a) 20 µm and (b) 40 µm.

of the particles indicated an aggregated form of spherical *Kp-AgNPs* and the typical diameter of the spherical AgNPs was observed to be in the range of 20, 50, and 100 nm. Fig. 11 (d) depicts the selected area electron diffraction pattern obtained from the spherical *Kp-AgNPs* thus exhibiting a clear ring-like pattern. The diffraction ring of *Kp-AgNPs* validated the face-centered cubic geometrical arrangement of Ag, which typically reveals the polycrystalline structure of *Kp-AgNPs* [34].

Biogenic synthesis of Ag nanoparticles has been described to contain many potent biomolecules that are endorsed by antimicrobial activities [59]. Most nanoparticles, especially silver nanoparticles, are equipped with benefits owing to their large surface-to-volume ratio and biological characteristics, which present a cutting edge in the metal-based synthesis of nanoparticles. *K. pinnata* is a medicinal plant with many health benefits owing to the presence of active phytoconstituents in its leaf extract [60]. A recent study [61] that aimed to synthesize AgNPs using *Plantago lanceolata* extract has increased considerable focus in the fields of nanotechnology and biomedicine. The AgNPs were effectively synthesized using an aqueous-crude extract obtained from *P. lanceolata* and were characterized to assess their antioxidant and biological properties. The presence of nano-particles was determined through color-shift, UV-Vis spectroscopy, atomic-force microscopy, and FT-IR analysis, revealing the involvement of bio-molecules *viz*. phenolic acid and flavonoids in the reduction of silver ions. SEM images show the formation of spherical particles with a size of 30 ± 4 nm (mean). The experimental results of these findings suggest that the AgNPs synthesized using *P. lanceolata* extract possess excellent bioactive properties and [62] advanced research can be employed in various biological applications in the future in this field. Similarly, our study aimed at the formation of Ag nanoparticles using the aqueous leaf extract of *K. pinnata,* which could have ecological benefits. Therefore, *Kp-AgNPs* have been proven to exhibit antibacterial properties by affecting the overall growth of bacteria. UV-visible spectrophotometric analysis has demonstrated the interface plasmonic mechanism, which is known to cause resonant peaks to form at various wavelengths in various nanoparticle solutions. According to a report by [63], black cumin is one of the most widely studied plants for its naturally occurring compounds with antimicrobial potential. A successful strategy for enhancing yield & quality in many crops is the use of foliar applications of growth stimulators. This study examined different treatments, including various moringa leaf extract concentrations (10% and 20%) and different growth stages as well as two controls: an un-sprayed check and a sprayed check. The results showed that the application of 20% moringa leaf extract after sowing significantly improved essential oil content, peroxidase value, iodine value branches per plant, fixed oil content, and plant height of black cumin oil compared to the un-sprayed control. Overall, the study demonstrated that the application of moringa leaf extract after sowing led to the greatest improvements in growth and yield of black cumin. Further research with various growth regulators, fertilizer combinations, and bio-stimulants is recommended to determine their synergistic effects and provide more acceptable and reliable recommendations in the future. In our study, this causes the maximum wavelength to be absorbed at the resonant wavelength, which may be due to

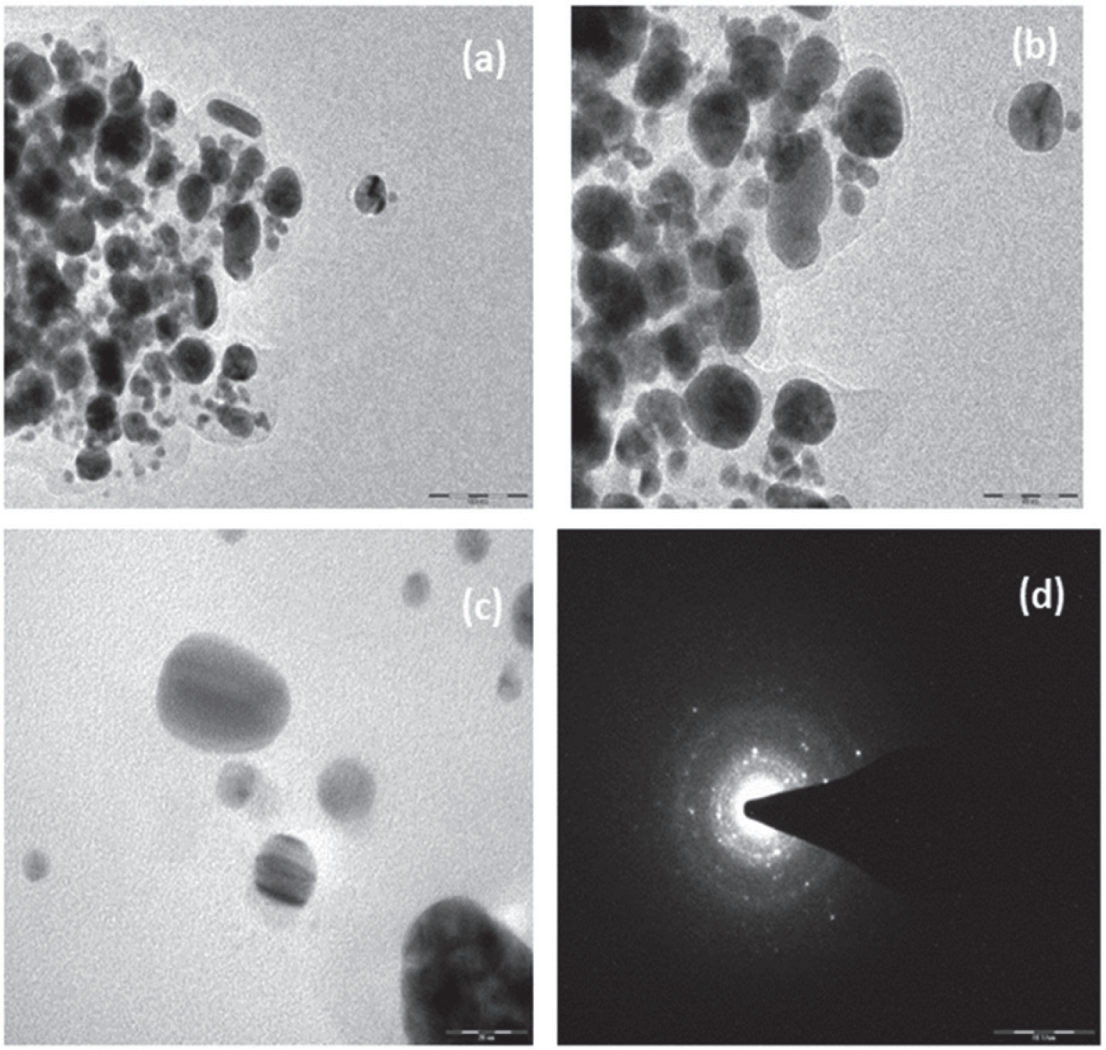

Fig. 11. TEM images of *Kp-AgNPs* (a): Size of nanoparticles 100 nm, (b) 50 nm, (c) 20 nm, and (d) SAED pattern of nanocrystalline Ag.

the nanoparticle structure and size formed in the solution. Hence, the peak observed at 400 nm indicates the reduction of Ag^{+} to Ag^{0} ions. This led to the inference that the reduction process occurred due to the existence of active metabolites in the leaf extract of *K. pinnata*. The FTIR spectrum showed the existence of carboxylic acid, amide groups, and several other protein excitations in the range of 3305.8 cm^{-1} and 1635.7 cm^{-1}. These results suggest that the detection of peaks in a particular range was due to the persistence of secondary metabolites, which act as capping agents and play a role in the stabilization of these particles. Therefore, it can be inferred that these compounds were crystalline. Size-distribution of the nanoparticles synthesized reveals the diameter of the nanoparticles in the range of 37.8 nm and 43.8 nm. This size demonstrates the stability of nanoparticles in colloidal suspensions. The zeta Potential analyzer reported the value of the silver nanoparticles to be of -26.7 mV which points towards the enhanced form of stability and the hydrodynamic distribution of the nanoparticles formed. Thus, the size offers an advantage in the long-term constancy of the particles and proves to be a better suspension for the fabrication process to follow in the near future. The SEM images show different morphological features of the nanoparticles. The morphology of the silver nanoparticles was found to have various forms, such as hexagonal, cuboidal, and rectangular forms of *Kp-AgNPs*. Such forms reveal the aggregated and dispersed forms of nanoparticles formed in the range of 40–20 µm. TEM images were used to evaluate the surface features, size, and morphology of the nanoparticles formed NPs. TEM was used to examine how silver nanoparticles interaction of AgNPs with bacterial cells. Upon addition of AgNPs nanoparticles the reduction in bacterial growth could have occurred because of the injury caused by the integrity of the bacterial cell and cytoplasm leakage. The typical

diameter of the *Kp-AgNPs* revealed the spherical form of the nanoparticles, as well as in the measurements at 20 nm, 50 nm, and 100 nm. Overall, the diffraction pattern also suggests the polycrystalline nature of *Kp-AgNPs*. Hence, the suggested environmentally friendly method could aid in the production of well-dispersed AgNPs from *K. pinnata* leaf extracts. This practical approach proved to be more effective than conventional methods. Furthermore, strategies and methods need to be assessed when discussing the toxicity imposed by these nanoparticles and suggesting ways to improve them so that in the future, they could be more efficiently used as capping agents in the biomedical sector.

Conclusions

The suggested environmentally friendly method for producing well-dispersed and antibacterial AgNPs from *K. pinnata* leaf extract offers a practical and effective methodology compared to conventional methods. This process is considerably simpler, reasonably priced, and environmentally friendly. The ethanolic extract of *K. pinnata* leaves contains secondary metabolites and organic acids such as alkaloids, flavonoids, glycosides, bufadienolide, steroids, lipids, and triterpenes. These metabolites serve as reducing agents, converting metallic ions into green nanoparticles and thus maintaining their stable form. As a result, they are components of green synthesis. Based on the FT-IR spectroscopy results, it is feasible to state that the metabolites and phenols found in *K. pinnata* help accelerate the conversion of Ag^{+} ions to Ag^{0}. Therefore, it can be understood from studies that AgNPs produced using environmentally friendly methods present a possible weapon against the spread of antibiotic resistance. The ideal conditions for the biosynthesis of AgNPs were achieved using the *K. pinnata* leaf extract. These metabolites serve as capping agents because they can convert metallic ions into green nanoparticles and stabilize them. Alkaline pH and higher temperatures were found to be more advantageous for the development of AgNPs after analyzing the consequences of a number of variables, including pH, temperature, reactant concentrations, and reaction duration. The synthesis of AgNPs occurred in 60 min, and this standard room-temperature environment was beneficial for the production of minor particles and the distribution of AgNPs was significantly affected by the initial concentration of the well. In addition to UV-visible absorption spectroscopy, the biosynthesized AgNPs were evaluated using SEM, differential light scattering, zeta-potential, and FTIR. As per the Differential Light scattering, the average size of the silver nanoparticle was found to be 19.75 nm and 347.47 nm, respectively. AgNPs nanoparticles been reported to be spherical. When subjected to bio-synthesized AgNPs, almost all selected organisms, including *S. aureus, P. aeruginosa* and *E. coli*, demonstrated increased antibacterial activity. Ag-NPs are excellent for biomedical applications and industrial settings where dye degradation is required, owing to their antibacterial properties.

Funding

This research was funded by Taif University, Saudi Arabia, Project No. (TU-DSPP-2024-10).

Acknowledgment

The authors are especially thankful to the Graphic Era (Deemed to be University), India, for allowing us to perform the research work in their laboratories to perform the analysis-related work in their laboratory. The authors extend their appreciation to Taif University, Saudi Arabia, for supporting this work through Project Number (TU-DSPP-2024–10).

Conflict of Interest

The authors declare no conflict of interest.

References

1. KHOJAH E., SAMI R., HELAL M., ELHAKEM A., BENAJIBA N., ALHARBI M., ALKALTHAM M.S. Effect of Coatings Using Titanium Dioxide Nanoparticles and Chitosan Films on Oxidation during Storage on White Button Mushroom. Crystals. **11**, 1, **2021**.
2. MALIK S., MUHAMMAD K., WAHEED Y. Nanotechnology: A revolution in modern industry. Molecules. **28** (2), 661, **2023**.
3. GIRI A.K., JENA B., BISWAL B., PRADHAN A.K., ARAKHA M., ACHARYA S., ACHARYA L. Green synthesis and characterization of silver nanoparticles using Eugenia roxburghii DC. extract and activity against biofilm-producing bacteria. Scientific Reports. **12** (1), 8383, **2022.**
4. GURUNATHAN S. Rapid biological synthesis of silver nanoparticles and their enhanced antibacterial effects against Escherichia fergusonii and Streptococcus mutans. Arabian Journal of Chemistry. **12** (2), 168, **2019**.
5. XU L., WANG Y.Y., HUANG J., CHEN C.Y., WANG Z.X., XIE H. Silver nanoparticles: Synthesis, medical applications and biosafety. Theranostics. **10** (20), 8996, **2020**.
6. DHAKA A., MALI S.C., SHARMA S., TRIVEDI R. A review on biological synthesis of silver nano-particles and their potential applications. Results in Chemistry. **6**, 101108, **2023**.
7. GUDIKANDULA K., CHARYA M.S. Synthesis of silver nanoparticles by chemical and bio-logical methods and their antimicrobial properties. Journal of Experimental Nanoscience. **11** (9), 714, **2016**.
8. MBA I.E., NWEZE E.I. Nanoparticles as therapeutic options for treating multidrug-resistant bacteria: Research progress, challenges, and prospects. World Journal of Microbiology and Biotechnology. **37**, 1, **2021**.

9. AFLAKIAN F., MIRZAVI F., AIYELABEGAN H.T., SOLEIMANI A., NAVASHENAQ J.G., KARIMI-SANI I., ZOMORODI A.R., VAKILI-GHARTAVOL R. Nanoparticles-based therapeutics for the management of bacterial infections: a special emphasis on FDA approved products and clinical trials. European Journal of Pharmaceutical Sciences. **188**, 106515, **2023**.
10. ADENIJI O.O., NONTONGANA N., OKOH J.C., OKOH A.I. The potential of antibiotics and nano-material combinations as therapeutic strategies in the management of multidrug-resistant infections: a review. International Journal of Molecular Sciences. **23** (23), 15038, **2022**.
11. MAMUN M.M., SORINOLU A.J., MUNIR M., VEJERANO E.P. Nanoantibiotics: Functions and properties at the nanoscale to combat antibiotic resistance. Frontiers in Chemistry. **9**, 687660, **2021**.
12. MORADI F., GHAEDI A., FOOLADFAR Z., BAZRGAR A. Recent advance on nanoparticles or nano-materials with anti-Multidrug resistant Bacteria and anti-bacterial biofilm properties; A systematic review. Heliyon. **9** (11), e22105, **2023**.
13. YILMAZ G.E., GÖKTÜRK I., OVEZOVA M., YILMAZ F., KILIÇ S., DENIZLI A. Antimicrobial nanomaterials: a review. Hygiene. **3** (3), 269, **2023**.
14. CHANDRAKALA V., ARUNA V., ANGAJALA G. Review on metal nanoparticles as nanocarriers: Current challenges and perspectives in drug delivery systems. Emergent Materials. **5** (6), 1593, **2022**.
15. AHMAD S.A., DAS S.S., KHATOON A., ANSARI M.T., AFZAL M., HASNAIN M.S., NAYAK A.K. Bactericidal activity of silver nanoparticles: A mechanistic review. Materials Science for Energy Technologies. **3**, 756, **2020**.
16. DAS B., DASH S.K., MANDAL D., GHOSH T., CHATTOPADHYAY S., TRIPATHY S., DAS S., DEY S.K., DAS D., ROY S. Green synthesized silver nanoparticles destroy multidrug resistant bacteria via reactive ox-ygen species mediated membrane damage. Arabian Journal of Chemistry. **10** (6), 862, **2017**.
17. RAY M.K., MISHRA A.K., MOHANTA Y.K., MAHANTA S., CHAKRABARTTY I., KUNGWANI N.A., AVULA S.K., PANDA J. PUDAKE R.N. Nanotechnology as a promising tool against phytopathogens: A futuristic approach to agriculture. Agriculture. **13** (9), 1856, **2023**.
18. BARROS C.H., FULAZ S., STANISIC D., TASIC L. Biogenic nanosilver against multidrug-resistant bacteria (MDRB). Antibiotics. **7** (3), 69, **2018**.
19. XIE J., LEE J.Y., WANG D.I., TING Y.P. Silver nanoplates: from biological to biomimetic synthesis. ACS Nano. **1** (5), 429, **2007**.
20. GAUTAM D., DOLMA K.G., KHANDELWAL B., GUPTA M., SINGH M., MAHBOOB T., TEOTIA A., THOTA P., BHATTACHARYA J., GOYAL R., OLIVEIRA S.M.R., PEREIRA M.D.L., WIART C., WILAIRATANA P., EAWSAKUL K., RAHMATULLAH M., SARAVANABHAVAN S.S., NISSAPATORN V. Green synthesis of silver nanoparticles using Ocimum sanctum Linn. and its antibacterial activity against multidrug resistant Acinetobacter baumannii. PeerJ. **11**, **2023**.
21. XU Z., DENG M. Identification and Control of Common Weeds: Volume 2, Identif. Control Common Weeds. **2** (2), 475, **2017**.
22. GUPTA R., LOHANI M., ARORA S. Anti-inflammatory activity of the leaf extracts/ fractions of Bryophyl-lumpinnatum Saliv. International Journal of Pharmaceutical Sciences Review and Research. **3**, 16, **2010**.
23. EKPO J.C., UDO E.S., TOM E.J., ARCHIBONG A.M., INYANG, I.P. Effects of ethanolic and aqueous leaf extracts of Bryophyllum pinnatum on haematological parameters of normal and streptozotocin–induced diabetic rats. Biokemistri. **33** (3), 181, **2021**.
24. YADAV M., GULKARI V., WANJARI M. Bryophyllumpinnatum leaf extracts prevent formation of renal calculi in lithiatic rats. Ancient Science of Life. **36**, 90, **2016**.
25. SOHGAURA A., BIGONIYA P., SHRIVASTAVA B. In-vitro antilithiatic potential of Kalanchoepinnata, Emblica of-ficinalis, Bambusanutans, and Cynodondactylon. Journal of Pharmacy and Bioallied Sciences. **10**, 83, **2018**.
26. RAFIQUE M., SADAF I., RAFIQUE M.S., TAHIR M.B. A review on green synthesis ofAgNPs and their applications, Artif. Cells, Nanomed. Biotechnol. **45**, 1272, **2017**.
27. MARCINIAK L., NOWAK M., TROJANOWSKA A., TYLKOWSKI B., JASTRZAB R. The effect of pH on the size of silver nanoparticles obtained in the reduction reaction with citric and malic acids. Materials. **13** (23), 5444, **2020**.
28. HANDAYANI W., NINGRUM A.S., IMAWAN C. The role of pH in synthesis silver nanoparticles using pometia pinnata (matoa) leaves extract as bioreductor. In Journal of Physics: Conference Series. **1428** (1), 012021, **2020**.
29. RAJAN R., CHANDRAN K., HARPER S.L., YUN S.I., KALAICHELVAN P.T. Plant extract synthesized silver nanoparticles: An ongoing source of novel biocompatible materials. Industrial Crops and Products. **70**, 356, **2015**.
30. ANTUNES F.S., DOS S.S., DOS A.L., BACKX B.P., SORAN M.L., OPRIŞ O., LUNG I., STEGARESCU A., BOUOUDINA M. Biosynthesis of nanoparticles using plant extracts and essential oils. Molecules. **28** (7), 3060, **2023**.
31. VANLALVENI C., LALLIANRAWNA S., BISWAS A., SELVARAJ M., CHANGMAI B., ROKHUM S.L. Green synthesis of silver nanoparticles using plant extracts and their antimicrobial activities: A review of recent literature. RSC Advances. **11** (5), 2804, **2021**.
32. JHA S.K., JHA A. Plant Extract Mediated Synthesis of Metal Nanoparticles, their Characterization and Applications: A Green Approach. Current Green Chemistry. **8** (3), 185, **2021**.
33. SIAKAVELLA I.K., LAMARI F., PAPOULIS D., ORKOULA M., GKOLFI P., LYKOURAS M., AVGOUSTAKIS K., HATZIANTONIOU S. Effect of plant extracts on the characteristics of silver nanoparticles for topical application. Pharmaceutics. **12** (12), 1244, **2020**.
34. IBRAHIM N.H., TAHA G.M., HAGAGGI N.S.A., MOGHAZY M.A. Green synthesis of silver nanoparticles and its environmental sensor ability to some heavy metals. BMC Chemistry. **18** (1), 7, **2024**.
35. ANSARI M., AHMED S., ABBASI A., KHAN M.T., SUBHAN M., BUKHARI N.A., HATAMLEH A.A., ABDELSALAM N.R. Plant mediated fabrication of silver nanoparticles, process optimization, and impact on tomato plant. Scientific Reports. **13** (1), 18048, **2023**.
36. VIJAYAKUMAR S., MALAIKOZHUNDAN B., SARAVANAKUMAR K., DURÁN-LARA E.F., WANG M.H., VASEEHARAN B. Garlic clove extract assisted silver nanoparticle – Antibacterial, antibiofilm, antihelminthic, anti-inflammatory, anticancer and ecotoxicity assessment. Journal of Photochemistry and Photobiology B: Biology. **198**, 111558, **2019**.

37. JAIN S., MOHAN S.M. Medicinal plant leaf extract and pure flavonoid mediated green synthesis of AgNPs and their enhanced antibacterial property. Scientific Reports. **7** (1), 1, **2017**.
38. BIANCHINI F.R., DOMINGUES R.J., LEMOS B.T.W., GONCALVES G.A.D., DE P.F., PRATAVIEIRA S., CHIAVACCI L.A., JUNIOR J.P.A., COSTA P.I.D., MARTINEZ L.R. Zinc-based nanoparticles reduce bacterial biofilm formation. Microbiology Spectrum. **11** (2), e04831, **2023**.
39. NAIDU S., SINGH I.K., SINGH A. Microbial Synthesis of Magnetic Nanoparticles for Plant Science and Agriculture. Plant Nano Biology. **4**, 100036, **2023**.
40. DIPIETRO R.S., JOHNSON H.G., BENNETT S.P., NUMMY T.J., LEWIS L.H., HEIMAN D. Determining magnetic nanoparticle size distributions from thermomagnetic measurements. Applied Physics Letters. **96** (22), 222506, **2010**.
41. SAMI R., KHOJAH E., ELHAKEM A., BENAJIBA N., HELAL M., ALHUTHAL N., ALZAHRANI S.A., ALHARBI M., CHAVALI M., Performance Study of Nano/SiO2 Films and the Antimicrobial Application on Cantaloupe Fruit Shelf-Life. Applied Sciences. **11**, 1, **2021**.
42. RAJA S., RAMESH V., THIVAHARAN V. Green biosynthesis of AgNPs using Calliandra haematocephala leaf extract, their antibacterial activity and hydrogen peroxide sensing capability. Arabian Journal of Chemistry. **10**, 253, **2017**.
43. IMALI A.M., ALAA A.M., VICKI H.G. ATR-FTIR Spectroscopy as a Tool to Probe Surface Adsorption on Nanoparticles at the Liquid-Solid Interface in Environmentally and Biologically Relevant Media. Analyst. **139** (5), 654, **2014**.
44. WAN W.K.A., SHAMELI K., JAZAYERI S.D., OTHMAN N.A., CHE N.W., HASSAN N.M. Biosynthesized silver nanoparticles by aqueous stem extract of Entada spiralis and screening of their biomedical activity. Frontiers in Chemistry. **8**, 620, **2020**.
45. AL-ZAHRANI S., ASTUDILLO-CALDERÓN S., PINTOS B., PÉREZ-URRIA E., MANZANERA J.A., MARTÍN L., GOMEZ-GARAY A. Role of synthetic plant extracts on the production of silver-derived nanoparticles. Plants. **10** (8), 1671, **2021**.
46. RAMON P., BERGMANN D., ABDULLA H., SPARKS J., OMORUYI F. Bioactive ingredients in K. pinnata extract and synergistic effects of combined K. pinnata and metformin preparations on antioxidant activities in diabetic and non-diabetic skeletal muscle cells. International Journal of Molecular Sciences. **24** (7), 6211, **2023**.
47. VILLARREAL W.L., ROBLES J.E., COSTA G.M. Phytochemical Standardization of an Extract Rich in Flavonoids from Flowers of Kalanchoe pinnata (Lam) Pers. Scientia Pharmaceutica. **91** (4), 50, **2023**.
48. KENDESON C.A., KAGORO M.L., ADELAKUN E.A. Phytochemical and pharmacological evaluation of Nigerian Kalanchoe pinnata (Lam.) stem-bark. Journal of Chemical Society of Nigeria. **46** (4), **2021**.
49. GHASEMPOUR A., DEHGHAN H., ATAEE M., CHEN B., ZHAO Z., SEDIGHI M., GUO X., SHAHBAZI M.A. Cadmium sulfide nanoparticles: preparation, characterization, and biomedical applications. Molecules. **28** (9), 3857, **2023**.
50. MAHMOUDI M. The need for robust characterization of nanomaterials for nanomedicine applications. Nature Communications. **12** (1), 5246, **2021**.
51. LIU H., ZHANG H., WANG J., WEI J. Effect of temperature on the size of biosynthesized silver nanoparticle: deep insight into microscopic kinetics analysis. Arabian Journal of Chemistry. **13** (1), 1011, **2020**.
52. AMALA S.E., NWEKE S.N., NWALOZIE R., MONSI T.P. Antimicrobial properties and phytochemical composition of Garcinia kola, Bryophyllum pinnatum, and Allium sativum juices on some clinical pathogens. Advances in Bioscience and Biotechnology. **12** (11), 388, **2021**.
53. LIAO C., LI Y., TJONG S.C. Bactericidal and cytotoxic properties of silver nanoparticles. International Journal of Molecular Sciences. **20** (2), 449, **2019**.
54. HASSAN A., ULLAH H. Antibacterial and antifungal activities of the medicinal plant veronica biloba. Journal of Chemistry. **5264943**, 1, **2019**.
55. URNUKHSAIKHAN E., BOLD B.E., GUNBILEG A., SUKHBAATAR N., MISHIG-OCHIR T. Antibacterial activity and characteristics of silver nanoparticles biosynthesized from Carduus crispus. Scientific Reports. **11** (1), 21047, **2021**.
56. PATRA J.K., BAEK K.H. Antibacterial activity and synergistic antibacterial potential of biosynthesized AgNPs against foodborne pathogenic bacteria along with its anticandidal and antioxidant effects. Frontiers in Microbiology. **8**, 167, **2017**.
57. LIAO C., LI Y., TJONG S.C. Bactericidal and cytotoxic properties of silver nanoparticles. International Journal of Molecular Sciences. **20** (2), 449, **2019**.
58. QING Y., CHENG L., LI R., LIU G., ZHANG Y., TANG X., WANG J., LIU H., QIN Y. Potential antibacterial mechanism of AgNPs and the optimization of orthopedic implants by advanced modification technologies, International Journal of Nanomedicine. **13**, 3311, **2018**.
59. ROZHIN A., BATASHEVA S., KRUYCHKOVA M., CHEREDNICHENKO Y., ROZHINA E., FAKHRULLIN R. Biogenic silver nanoparticles: Synthesis and application as antibacterial and antifungal agents. Micromachines. **12** (12), 1480, **2021**.
60. VILLARREAL W.L., ROBLES J.E., COSTA G.M. Phytochemical Standardization of an Extract Rich in Flavonoids from Flowers of *Kalanchoe pinnata* (Lam) Pers. Scientia Pharmaceutica. **91** (4), 50, **2023**.
61. SHAH M.Z., GUAN Z.H., DIN A.U., ALI A., REHMAN A.U., JAN K., FAISAL S., SAUD S., ADNAN M., WAHID F., ALAMRI S. Synthesis of silver nanoparticles using *Plantago lanceolata* extract and assessing their antibacterial and antioxidant activities. Scientific Reports. **11**, 20754, **2021**.
62. KHAN S.U., KHAN M.S., WANG H., QIAN M., JAVED T., FAHAD S., LU K. Harnessing nanobiotechnology for drought stress: transforming agriculture's future; what, why and how? Environmental Science: Nano. **7**, **2024**.
63. ABID M., KHALID N., QASIM A., SAUD A., MANZER H.S., CHAO W., DEPENG W., SHAH S., JAN B., SUBHAN D., RAHUL D. Exploring the potential of moringa leaf extract as bio stimulant for improving yield and quality of black cumin oil. Scientific Reports. **11**, 24217, **2021**.